Optical and UV properties of jetted active galactic nuclei

Alice Deconto Machado[1], Ascensión del Olmo Orozco[1], Paola Marziani[2]

[1]Instituto de Astrofísica de Andalucía, IAA-CSIC, Granada, Spain
[2]INAF, Osservatorio Astronomico di Padova, Italia

Much effort has been done in order to better understand the active galactic nuclei mechanisms behind the relativistic jets observed in radio-loud sources. These phenomena are commonly seen in luminous objects with intermediate/high redshift such as quasars, so that the analysis of the spectroscopic properties of these sources may be a way to clarify this issue. Measurements are presented and contextualized taking advantage of the set of correlations associated with the quasar Main Sequence (MS), a parameter space that allows to connect observed properties to the relative relevance of radiative and gravitational forces. In the redshift range we consider, the high-ionization lines in the UV in the quasar rest-frame are redshifted into the optical domain, while the low-ionization HI Balmer line Hβ is shifted into the near IR. Observations covering the Hβ spectral region were collected with the IR spectrometer ISAAC at ESO-VLT. They make it possible to obtain an accurate measurement of the quasar rest-frame and to set the location of a quasar along the MS. In addition, the knowledge of the rest-frame allows for a quantitative comparison between low- and high-ionization lines. The comparison between the strong CIVλ1549 high-ionization line and Hβ in terms of line widths and shifts with respect to rest-frame leads to an evaluation of the role of radiative forces in driving an accretion disk wind. While for non-jetted quasars the wind properties have been extensively characterized as a function of luminosity and other physical parameters, the situation is by far less clear for jetted sources. The overarching issue is the effect of the relativistic jet on the wind, and on the structure of the emitting region in general. We present preliminary results and examples of our analysis of the optical line profiles aimed to identifying the wind contribution to the line emission.

The Quasar Main Sequence (MS)

Sulentic et al. 2000 proposed a correlation space, the so-called **4D eigenvector 1** parameter space (4DE1) that involves parameters from the optical and UV emission lines, and from the soft-X ray domain.

The quasar MS is often illustrated by the distribution of the quasars in the 4DE1 optical plane FWHM of Hβ broad component versus FeIIλ4570Å strength, parametrized by R(FeII)= I(FeIIλ4570)/I(Hβ) (Sulentic et al. 2000; Marziani et al. 2018).

Eddington ratio, λ_E = L_{Bol}/L_{Edd}, and **orientation** are thought to be the **main physical drivers of the MS** (Marziani et al. 2001; Shen & Ho 2014; Sulentic et al. 2017).
Pop. B quasars are the ones with high black hole mass (M_{BH}) and low λ_E and **Pop. A** are fast-accreting with relatively small M_{BH} .

The MS shape on the figure below allows for the subdivision of quasar samples into 2 populations, Pop. A & B, and into a grid of bins of FWHM(Hβ) and FeII which defines a sequence of Spectral Types (ST). For low redshift sample (z < 1) the two population and the STs are defined as:

1) **Population A with FWHM(Hβ) ≤ 4000 km/s, and with ST defined by increasing R(FeII) from A1 with R(FeII) < 0.5 to A4 with 1.5 ≤ R(Fe II) ≤ 2;**

2) **Population B with FWHM(Hβ) > 4000 km/s, and ST bins defined in terms of increasing ΔFWHM(Hβ) = 4000 km/s.**

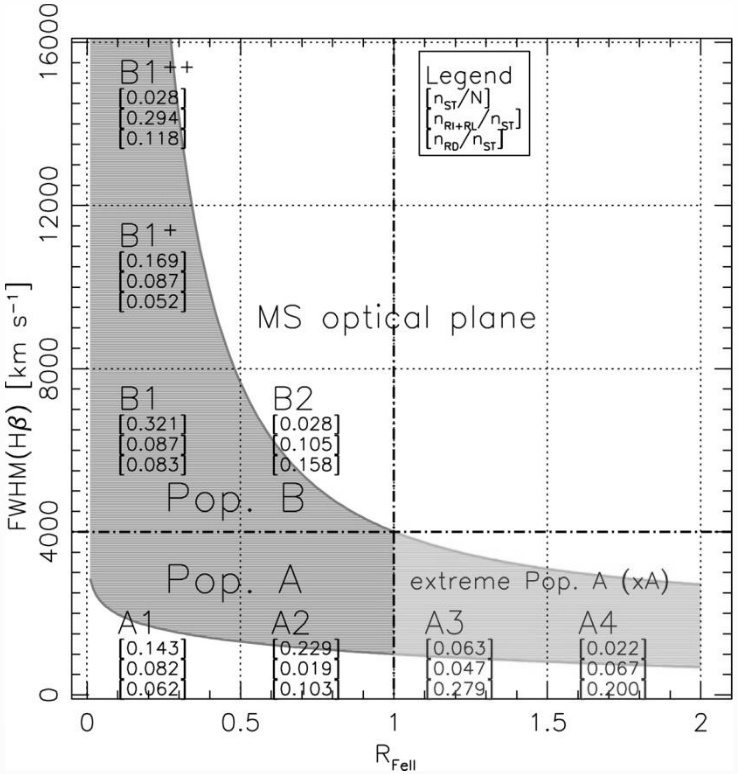

Radio-Loud quasars **are not distributed uniformly along the MS** (Zamfir et al. 2008; Ganci et al. 2019). They are predominantly found in the Pop. B domain, having R(FeII) < 0.5 and FWHM(Hβ) > 4000 km/s.

Sample

The sample consists of **36 high-luminosity QSOs** with **z = 1.4 - 3.8**, covering both **radio-loud** and **radio-quiet** sources.

All NIR spectra were obtained with the **ISAAC spectrograph at the VLT** with a slit width of 0.6 arcsec. The spectrum of each object corresponds to the λ range of an IR window (J, H, K) covering the region of redshifted Hβ and FeIIλ4570 (or FeIIλ5130 blend).

Matching rest-frame UV spectra were collected from the SDSS for 17 objects and with new observations with the ALFOSC spectrograph in the NOT 2.5m telescope at the Observatorio del Roque de los Muchachos (La Palma, Spain).

Multicomponent Fitting of the Hβ region

For the Hβ data analysis, we use a **non-linear multicomponent fitting including the continuum (a power law), a semi-empirical scalable FeII emission template and the emission line components**. The broad profile of the Hβ has been modeled by 3 main components:

- **A broad component (BC)** symmetric and unshifted profile (Lorentzian for Pop. A or Gaussian for Pop. B), associated with the virialized Broad Line Region (BLR);
- **A blueshifted component (BLUE)**, present mainly in **Pop. A** quasars, that has been modeled by one or more normal distributions;
- **A very broad Gaussian redshifted component (VBC)** clearly observed in **Population B** quasars (Wolf et al. 2020; Sulentic et al. 2017).

In addition, we included a **narrower component (NC)** superimposed to the broad emission line profile. The minimum χ^2 multicomponent fit was carried out with the SPECFIT routine in IRAF (Kriss 1994) yielding FWHM, peak wavelength, and intensity for all line components.

Analysis & Preliminary Results

We present the multicomponent fittings for one Pop. A and one Pop. B in the regions of **Hβ+[O III]λλ4959,5007** (left plot) and the **1900Å blend** (right plot), which includes AlIIIλ1860, SiIII]λ1892, CIII]λ1901 and FeIII emission lines (del Olmo et al., in preparation).

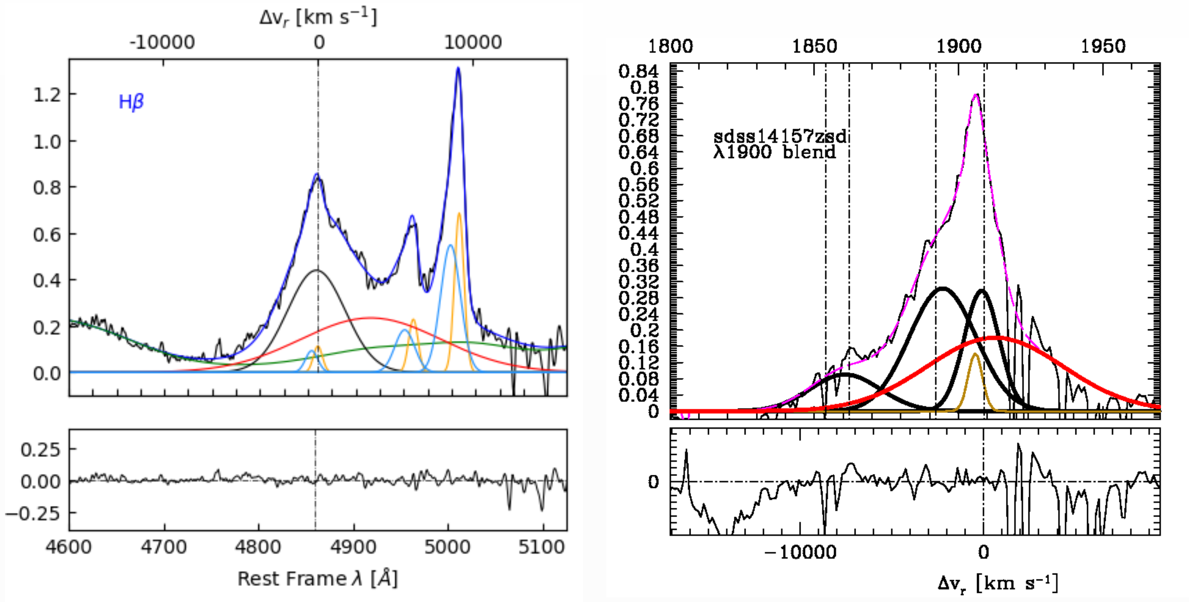

As a Pop. B object, all the components of SDSS J141546.24+112943.4 are fitted as Gaussians. The full Hβ profile is well represented by a NC and a BC at rest-frame and a VBC strongly shifted to the red with a FWHM > 10000 km/s.

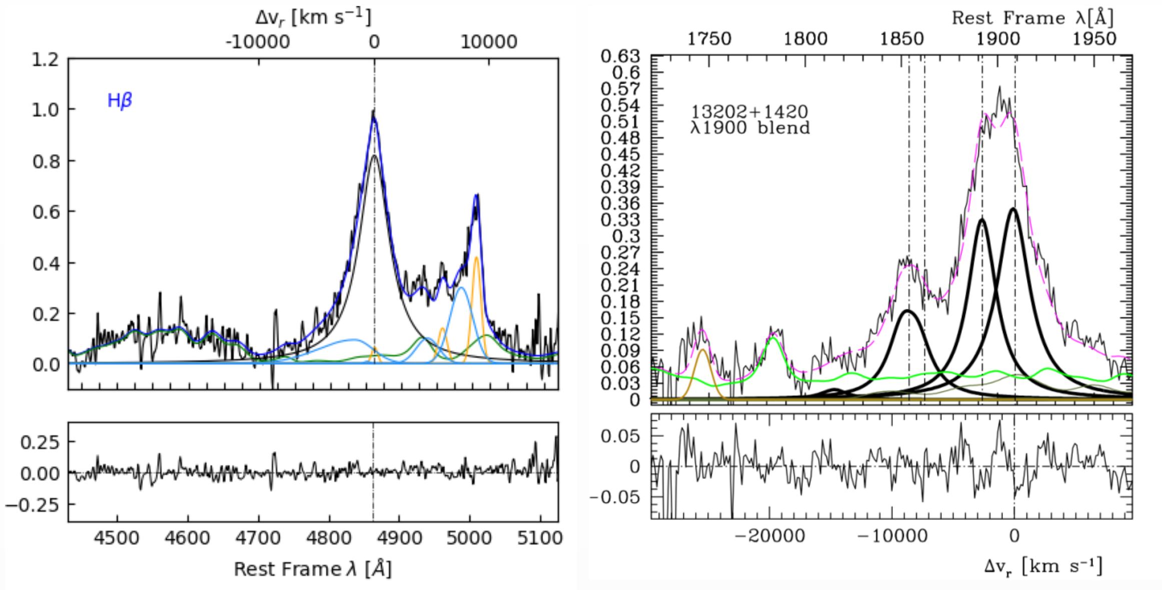

In the case of SDSS J132012.33+142037.1, the Hβ BC is well represented by a Lorentzian profile with a FWHM of 3224 km/s, while all the others components are treated as simple Gaussians. In order to represent the full Hβ profile, we have also to consider a blueshifted BC with a FWHM of 7519 km/s and a assimetry of 0.5, as well as small and blueshifted NCs at rest-frame.

These same procedures were done to the other reduced spectra from the sample. 54.5% of the sample were better fitted as Pop. B.

Analysis & Preliminary Results

Since we obtain FWHM(Hβ) and R(Fe II) from the SPECFIT fittings, we can also locate our objects along the quasar Main Sequence:

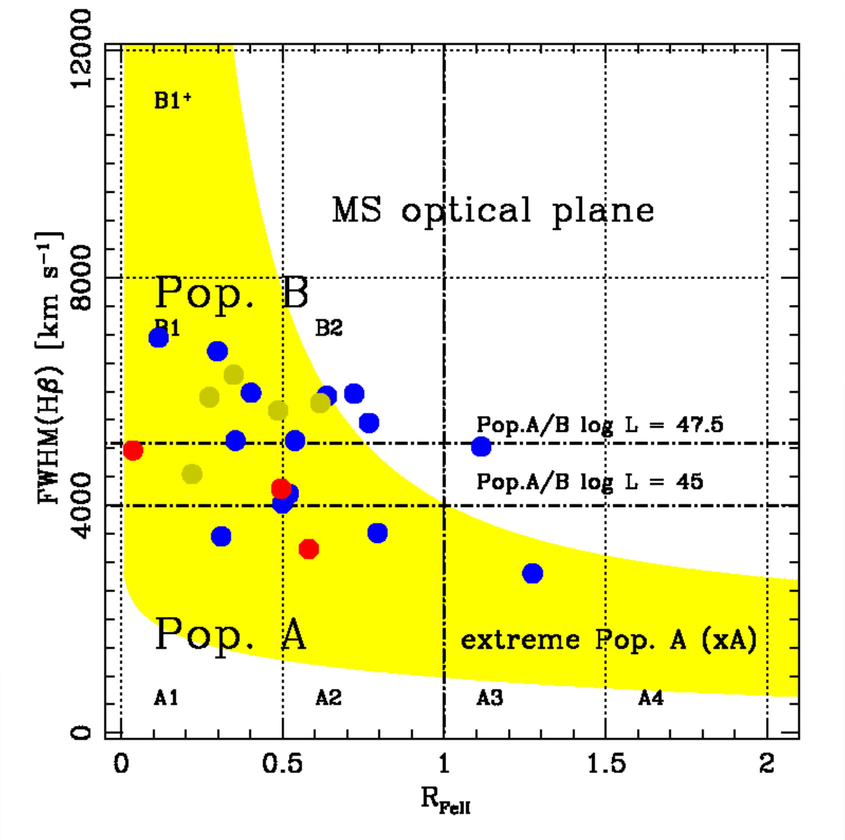

We estimate some physical parameters for the 22 objects, as the black hole mass (M_{BH}) and Eddington luminosity. M_{BH} was determined following the scaling law by Vestergaard and Peterson (2006):

$$\log M_{BH} = \log\left[\frac{FWHM(H\beta)}{1000\,\mathrm{km\,s^{-1}}}\right]^2 \left[\frac{\lambda L_\lambda(5100\text{Å})}{10^{44}\,\mathrm{erg\,s^{-1}}}\right]^{0.50} + (6.91 \pm 0.02),$$

in which FWHM(Hβ) includes only the Hβ BC. A histogram containing the M_{BH} estimates is presented below.

By retrieving information about the radio fluxes in surveys such as FIRST and NVSS, we estimate the radio loudness parameter, defined as:

$$R_L = \frac{f_{radio}}{f_{optical}}.$$

We found that 8 objects from our sample are radio-loud sources, while the others present low R_L.

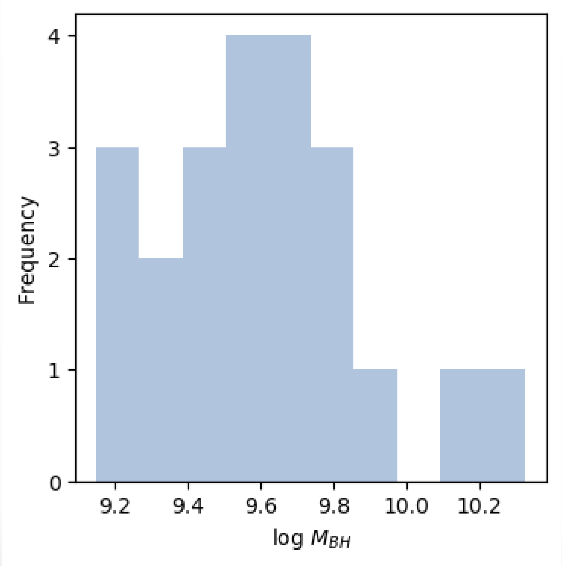

Ongoing Work & Perspectives

We have been studying 22 sources in the optical region using the IRAF SPECFIT tool to obtain multicomponent fits of the Hβ and [O III]λλ4959,5007, FeII, and other emission lines.

The next step will include the completion of the analysis in the optical, by reducing the data and fitting the reduced spectra of the missing objects. We also intend to discuss the behaviour of the sample in the UV region.

We are confident to be able to carry out a systematic comparison between RL and RQ quasars at high redshift taking advantage of the UV region emission lines that provide a powerful diagnostic tool to constrain the physical conditions of the Broad Line Region.

References

Ganci V., Marziani P., D'Onofrio M., del Olmo A., Bon E., Bon N., Negrete C. A., 2019, A&A, 630, A110
Kriss G., 1994, ASPC, 61, 437, ASPC...61
Marziani P., Del Olmo A., D'Onofrio M., Dultzin D., 2018, FrASS, 5, 28
Marziani P., Sulentic J. W., Negrete C.~A., Dultzin D., Zamfir S., Bachev R., 2010, MNRAS, 409, 1033
Marziani P, Sulentic J.W., Plauchu-Frayn I. & del Olmo A., 2013, A&A 555, A89
Marziani P., Sulentic J.W., Stirpe G.M., Zamfir S. & Calvani M., 2009, A&A 495,83
Marziani P., Sulentic J.W., Zwitter T., Dultzin-Hacyan D. & Calvani M., 2001, ApJ 558,553
Shen Y. & Ho L.C., 2014, Nature, 513, 210
Sulentic J. W., Del Olmo, A., Marziani P. et al., 2017, A&A, 608, A122
Sulentic J. W., Zwitter T., Marziani P., Dultzin-Hacyan D., 2000, ApJL, 536, L5
Vestergaard M., Peterson B. M., 2006, ApJ, 641, 689
Wolf J., Salvato M., Coffey D., et al., 2020, MNRAS, 492, 3580
Zamfir S., Sulentic J. W., Marziani P., 2008, MNRAS, 387, 856

A.D.M. acknowledges the support of the INPhINIT fellowship from "la Caixa" Foundation (ID 100010434). The fellowship code is LCF/BQ/DI19/11730018. A.D.M. and A.d.O. acknowledge financial support from the Spanish Ministry of Economy and Competitiveness through grant AYA2016-76682-C3-1-P and from the State Agency for Research of the Spanish MCIU through the "Center of Excellence Severo Ochoa" award for the Instituto de Astrofísica de Andalucía (SEV-2017-0709).